

Nano and Micro Ceramic Membranes from Degradable Templates

Neftalí Lenin Villarreal Carreño^{a}, Cristiane Wienke Raubach Rattman^a, Margarete Regina Freitas Gonçalves^a, Ricardo Marques e Silva^a, Gian Francesco dos Reis Paganotto^a, José Carlos Bernedo Alcazar^a, Cesar Oropesa Avellaneda^a, Ananda Morais Barbosa^a, Viviane Coelho Duarte^a, Poty Rodrigues de Lucena^b*

^aGraduated Program Science and Material Engineering, Technology Development Center – CDTEC, Federal University of Pelotas – UFPEL, Pelotas, RS, Brazil

^bCenter of Exact Sciences and Technology, Western Bahia Federal University – UFOB, Barreiras, BA, Brazil

Received: October 2, 2015; Revised: May 17, 2016; Accepted: July 8, 2016

The nano/microstructures with highly porous surface area have attracted tremendous attention, particularly the synthesis and tailoring of porous and hollow materials of high performance. In this paper, an easy method of cost-effective synthesis of hollow ceramic fiber membranes based on Hydroxyapatite, TiO₂ and ZrO₂ stabilized with Yttrium, is proposed by a single chemical route (polymeric precursor method) and a bio-template route (easy to degrade in thermal conditions). This article reports also the ZrTiO₄ nanowires synthesis on a silicon (100) wafer in a single step deposition/thermal treatment. Template-directed membrane synthesis strategy was associated to the polymeric precursor route and spin-coating deposition technique. In this method, ZrTiO₄ nanowire ceramic were synthesized by spin-coating thermal treatment technique using polycarbonate membrane as a template. According to the results, after heat-treatment by the template removal, the ZrTiO₄ nanowire consists of uniformly deposited crystalline and porous nanoparticles that exhibited a higher surface area and a higher porosity. The polycrystalline nanowires were obtained at by thermal treatment with diameter in the range of 60-100 nm. Photoluminescence spectra were collected for fiber at room temperature. These characterizations demonstrate the morphology of structures formed, showing its hollow and porous conformation, suitable applications to advanced reinforced or device component material.

Keywords: *Hollow fiber ceramic, porous material, photoluminescence and Nanowire*

1. Introduction

The biotemplating is a new concept to fabricate ceramic materials with novel hierarchical and complex microstructures using natural materials as templates¹, posterior conversion of its tissue to ceramic materials has attracted considerable interest due to the possibility of development and optimization of tailoring porous of this materials, which have been made by modification of raw material, appropriated selection of many different species templates, chemical compositions and other physical-chemical conditions to lead to desired materials, retaining the micro-morphologies of their original counterparts. The design of materials tailored porosity exhibit special properties and features that usually cannot be achieved by their conventional dense analogous. Additionally, porous materials find many applications as final products and in several technological processes. Macroporous materials are used in various forms and compositions in routinely day, including for instance polymeric foams for packaging, aluminum light-weight structures in buildings and airplanes, as well as porous ceramics for water purification. The

applications of porous ceramics material have appeared in the last decades, especially for environments where high temperature, extensive wear and corrosive media are involved. Such applications include, for example, the high-temperature thermal insulation, support for catalytic process, and filtration of hot corrosive gases in several industrial processes^{2,3}.

Membrane template-based synthesis of oxide nanostructures can be carried out by filling the porous surface of various polymeric or oxide membrane substrates with precursor solutions⁴⁻⁷, such as cellulose acetate, polycarbonate (PC), PVDF, PTFE and anodized alumina oxide (AAO) nano membranes⁸. AAO and PC membranes are conveniently used for the growth of nanostructures from various chemical and/or physical synthesis strategies⁹⁻¹¹. The diameter and length of the nanostructures obtained can be controlled by the pore size and thickness of the template membrane, but the elimination of the membrane is dependent of certain experimental conditions. Although oxide nanostructures have been grown applying chemical methods, the experimental conditions have strongly limited the compositions to monometallic oxides such as ZnO, SnO₂, In₂O₃ or TiO₂¹².

* e-mail: neftali@ufpel.edu.br

No study has previously been devoted to the synthesis of $ZrTiO_4$ oxide nanorods, nanowires, nanotubes or new 1D nanomaterials. The removal of the AAO (Al_2O_3) template membrane can be conducted by acid or basic chemical etching. Further polycarbonate membranes can be removed by heat treatment at moderate temperatures or dissolution with organic solvents, maintaining the desired oxide composition after removal¹².

There are varieties of methods to obtain precursor resins, among them, the Pechini method or polymeric precursors method has been extensively used in the synthesis of a variety of mono, bi and multimetallic oxides. The experimental simplicity and reproducibility of the methods, combined with the stoichiometric rigor in the synthesis of metal oxide compositions, especially in oxides comprising two or more metals, have increased their field of application to the synthesis of ferroelectric solid-solutions, photoluminescent powders, magnetic materials, superconductors, nanoparticles and photovoltaic materials. In this synthesis strategy, metallic cations linked to ester chains can be easily obtained through a condensation reaction under acid catalysis conditions¹³.

In this paper, the authors show an alternative method approach of organic templates method to obtain fiber hollow membranes by infiltrated process. This infiltration is performed by the use of a polymeric resin. Also in this study, bimetallic oxide nanowires were prepared using a template- directed method that combines the polymeric precursor method modified with a spin coating technique. Cellulose Nitrate membrane, cotton fiber, carton and natural sponge were used as a degradable template to obtain Hydroxyapatite, TiO_2 and ZrO_2 . Further proceeding from PC membrane were used to synthesis $ZrTiO_4$ nanowire oxide (ZT-nw) integrated into a silicon substrate. The aim of this article is to display a method and chemical route for the preparation of nano and micro ceramic materials.

2. Method and Procedure

2.1. Chemical Synthesis of ceramic fiber membranes at different compositions

Firstly, the resins were obtained from metallic cations (Ca, Ti or Zr) by a polymeric precursor method (Pechini method). This method is based on the chelation of cations (metals) by citric acid (CA), in a water solution containing metallic citrate. Chemical process consists of the formation of a M-citrate complex (M = Metallic: Ca, Ti or Zr), followed by a polymerization step with the addition of ethylene glycol (EG) to the metal/citrate solution, at a mass ratio of 40:60 in relation to the citric acid¹⁴.

2.2. Route to synthesis of Hydroxyapatite fibers

Calcium nitrate and ammonium phosphate dibasic purchased from Synth were mixed at 80 °C to complete

homogenization and stirred with CA (Aldrich), to posterior addition of EG (Aldrich). A CA/metal ratio of 4:1 (mol) was used. The viscosity of the resin was kept between 2.0 - 4.0 mPa•s, Brookfield viscometer DV-II+Pro was used to test the viscosity of resins.

The resin obtained was subsequently deposited onto cellulose acetate filter (pore diameter of 0.2 μ m, Sartorius Stedim Biotech GmbH 37070, Gottingen, Germany) by means of a spin coating technique, selected due to the high uniform deposition obtained through this method. Then, the material was subjected to heat treatment for two hours at 800 °C in air atmosphere, as illustrated in flowchart Figure 1.

2.3. Route to synthesis of TiO_2 fibers

The precursor resin used to synthesize TiO_2 was obtained by addition of citric acid to titanium isopropoxide (Across) in proportion of 3:1. Distilled water was added to the mixture and the reagents were dissolved by heating (150 °C) and stirring. Later, EG (Aldrich) was added to the solution. A CA/metal ratio of 3:1 (mol) was used. The viscosity of the resin varied between 3.0-5.0 Mpa.

The ceramic fibers were obtained by the calcination process at different treatment temperature, such as 600 °C, 800 °C, and 1000 °C at room atmosphere.

2.4. Route to synthesis of ZrO_2 fibers stabilized with Yttrium

Zirconium dichloride (Aldrich) and yttrium oxide (Aldrich) were used for the synthesis of ZrO_2 fibers stabilized with Yttrium, (0.9 mol of Zr and 0.1 mol of Y). The metallic citrate was prepared at 70 °C to complete homogenization and stirred with CA, to posterior addition of EG. This was followed by the liquid infiltration of the fibers on the biotemplate. The infiltration was carried out by dropping the precursor resin on the biotemplate by single capillary process; in this method thin strings of cotton, carton, piece of cloth of cotton and natural sponge were employed to prepare the hollow ceramic fiber membrane. The template impregnated with the resin was treated at 90 °C for 24 h in an air atmosphere, with posterior annealing treatment at temperatures of 800 °C and 1000 °C in air atmosphere for 3 h. The result is a hollow fiber material containing several sizes as functions of biotemplate matrix and thermal treatment¹⁵.

2.5. Route to synthesis of $ZrTiO_4$ nanowire ceramic

The nanowire of $ZrTiO_4$ are prepared through the single-step deposition/thermal treatment technique. In this method, stoichiometric amount of metallic citrate of Ti and Zr were dissolved in distilled water and methanol. To

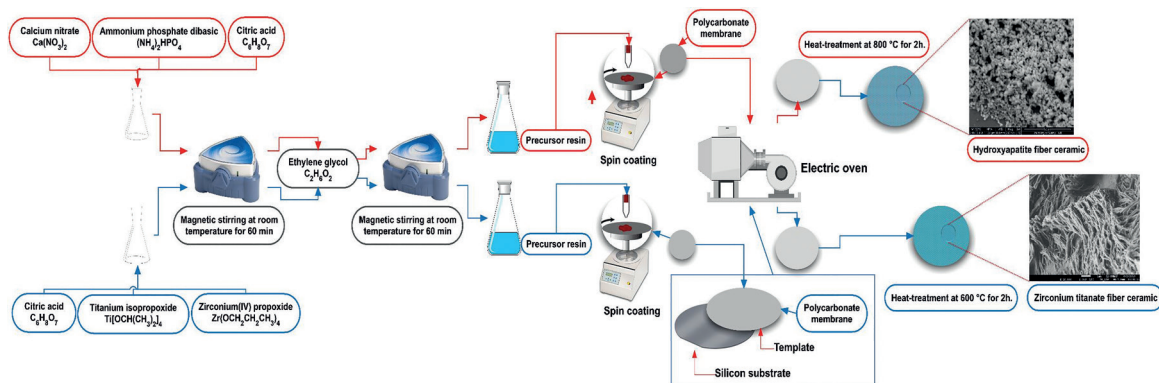


Figure 1. Schematic illustration of sample preparation of Zirconium titanate (ZrTiO_4) and Hydroxyapatite fiber ceramic.

get the precursor complex, the stoichiometric solutions of Ti and Zr were mixed to obtain the polymeric precursor ZrTiO_4 . The polymeric precursor was then coated onto polycarbonate membranes substrates adapted with millex filter syringe millipore at a spin rate of 7000 rpm for 20 s, using commercial spinner (Chemat Technology) model KW-4A, illustrated in Figure 1. The millex filter syringe Millipore was used in order to remove the excess of polymeric precursor solution. The silicon substrate was cleaned with 4:1 v/v $\text{H}_2\text{SO}_4:\text{H}_2\text{O}_2$ solution. After coating the membrane, polycarbonate were put onto silicon substrate and exposed to a heat treatment at 350°C for 2 h in EDG model 3000.

The thermal treatment of the impregnated PC membrane attached to the silicon substrate was performed in an electric oven under air atmosphere at a heating rate of $5^\circ\text{C}/\text{min}$ in two temperature steps: the first at 350°C for two hours for the organic matter pyrolysis, and the second at 700°C for two hours to obtain the nanowire oxide structure. A ZrTiO_4 powder sample was obtained with the same precursor solution under identical thermal treatment conditions for crystalline phase comparison¹⁶.

2.6. Characterization

The structural analysis of the hollow ceramic fiber membranes was carried out by the X-ray diffraction (XRD) patterns of the samples, that were obtained using a X-ray powder diffractometer (XRD-6000, Shimadzu, Japan) 30 kV and 20 mA, using $\text{CuK}\alpha$ radiation ($\lambda = 1.5418 \text{ \AA}$) with 2θ angle scanning from 20 – 80° , with steps of 0.5° , operating at room temperature. The structure and morphology of the samples was studied by Scanning Electron Microscopy (SEM; Shimadzu, model SSX-550) equipped with X-ray energy dispersive spectroscopy (EDS) and Transmission Electron Microscopy (TEM; Philips, model CM200, operated at 200 kV). Specific surface area of the nanocomposites was determined by an Autosorb-1C analyzer (Quantachrome Instruments). Energy Dispersive

X-ray Fluorescence Spectrometer (EDX, 720, Shimadzu) determined the chemical concentration of all tin samples, after heat treatment. Photoluminescence spectra were collected for fibers at room temperature by Thermal Jarrell-Ash Monospec 27 monochromator with the nominal output power of the laser kept at 350 mW.

The ceramic fibers were characterized by Field Emission Gun Scanning Electron Microscopy (FESEM), and EDS was performed for direct morphological and microstructural characterization of the sample with a silver electrical contact connected to the aluminum microscope support.

3. Result and Discussion

The SEM images and crystal structure of the ceramic membranes and the respective patterns are presented in Figure 2. The X-ray diffraction pattern of TiO_2 membranes as a function of the annealing temperature is illustrated in Figure 2b. In this pattern the peaks can be ascribed to the tetragonal rutile phase of crystalline TiO_2 . The tetragonal rutile phase was formed during the annealing of TiO_2 samples in temperatures between 600 and 800°C , however, the complete formation of rutile phase just was observed at sample using high temperature above 800°C . These observations corroborate with literature for titania powder, rutile transformation takes place at around 780°C , material derived of sol-gel process¹⁷.

The Figure 3 illustrates the SEM images and XRD pattern of ZrO_2 stabilized with Yttrium membrane (YSZ) annealed at 800°C , a having a grid format as template. The XRD patterns of this membranes (Figure 3C), also show that the crystalline phase is more evident in the fibers that the material with grid format in similar thermal condition, this can be attributed to the nature of template precursor that drive material with arrange specific and porous, Yang and Ma have described a method to obtain macroporous network structure based on crystalline ZrO_2 tube, from sol-gel mineralization membranes template and subsequent calcination¹⁸, then

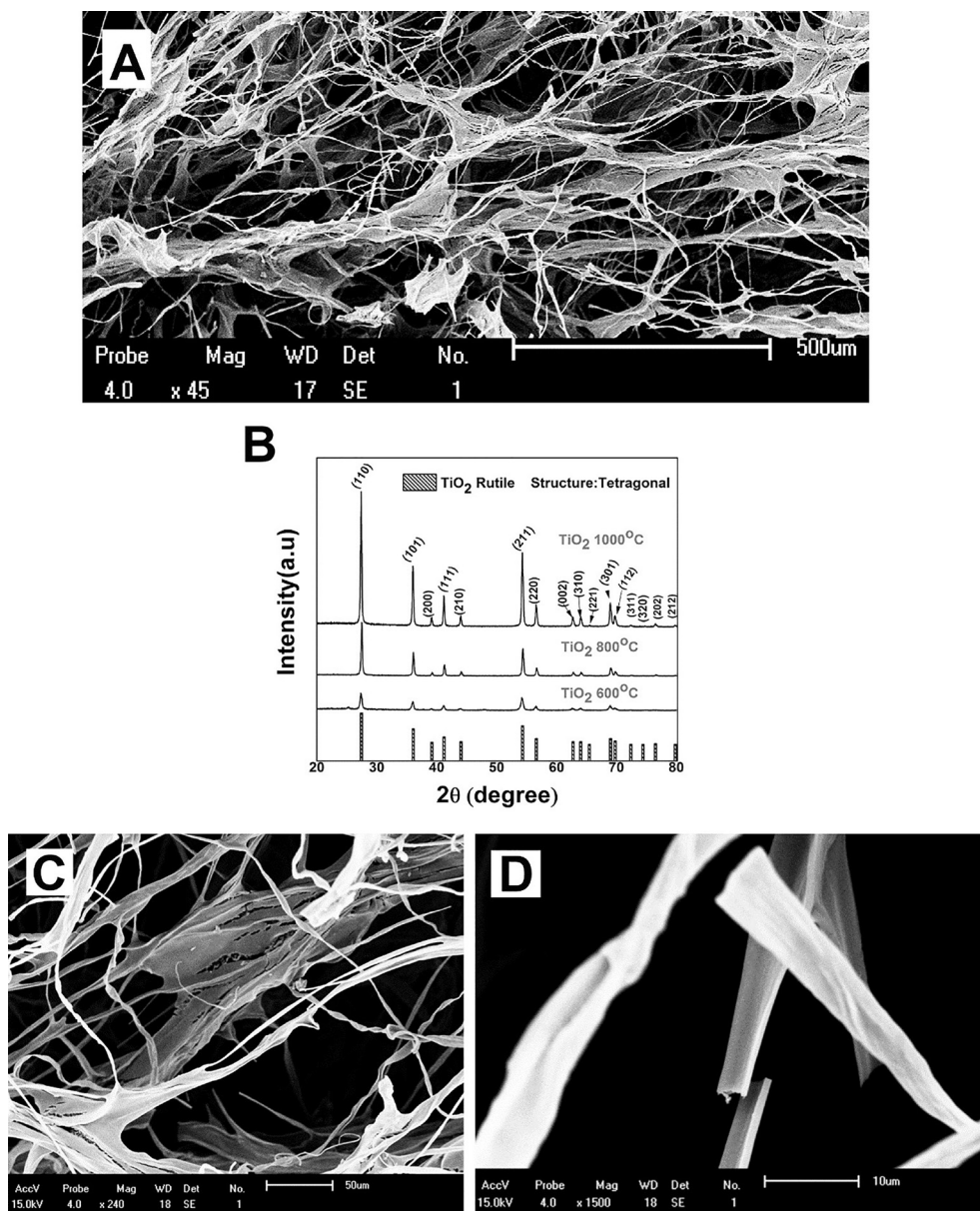


Figure 2. (A)(C)(D) SEM micrograph image of TiO₂ membrane at 600 °C and (B) XRD pattern of TiO₂ at different heat treatment (600 °C), (800 °C) and (1000 °C).

it suggest that several parameters (precursor and thermal treatment) can monitored and manipulated in order to control of final crystalline microstructure, thermogravimetry studies are in progress. Table 1, display the N₂ adsorption/desorption isotherms study, where a significant change of specific surface area and porous morphology were observed on YSZ membrane, after annealing samples at 1000 °C, grid YSZ membrane display mesoporous surface, thus the comparative surface analysis could be suggest that porous surface on membranes sample are dependence of original biodegradable template, additionally the role of template was observed in the preliminary study of PL at room temperature of samples illustrated in Figures 4a-b shows the photoluminescence

(PL) at room temperature of the fiber and grid membrane annealed at 1000 °C respectively (grid and fiber membranes show high crystalline phase). There experimental studies showing that cannot be observed PL emission of materials having high crystallization, but in this case, the presence of morphological structures hollow (here observed just for mesoporous material) profile in a sample may be responsible for significant emission photoluminescence¹⁴.

The Figure 5a-d illustrates the SEM images and XRD pattern of hydroxyapatite annealed at 600 °C for 3 h with piece card, fiber cotton (hollow) and grid shape as template, respectively. The XRD patterns of these membranes (Figure 5e), shows the low degree of crystallinity of the

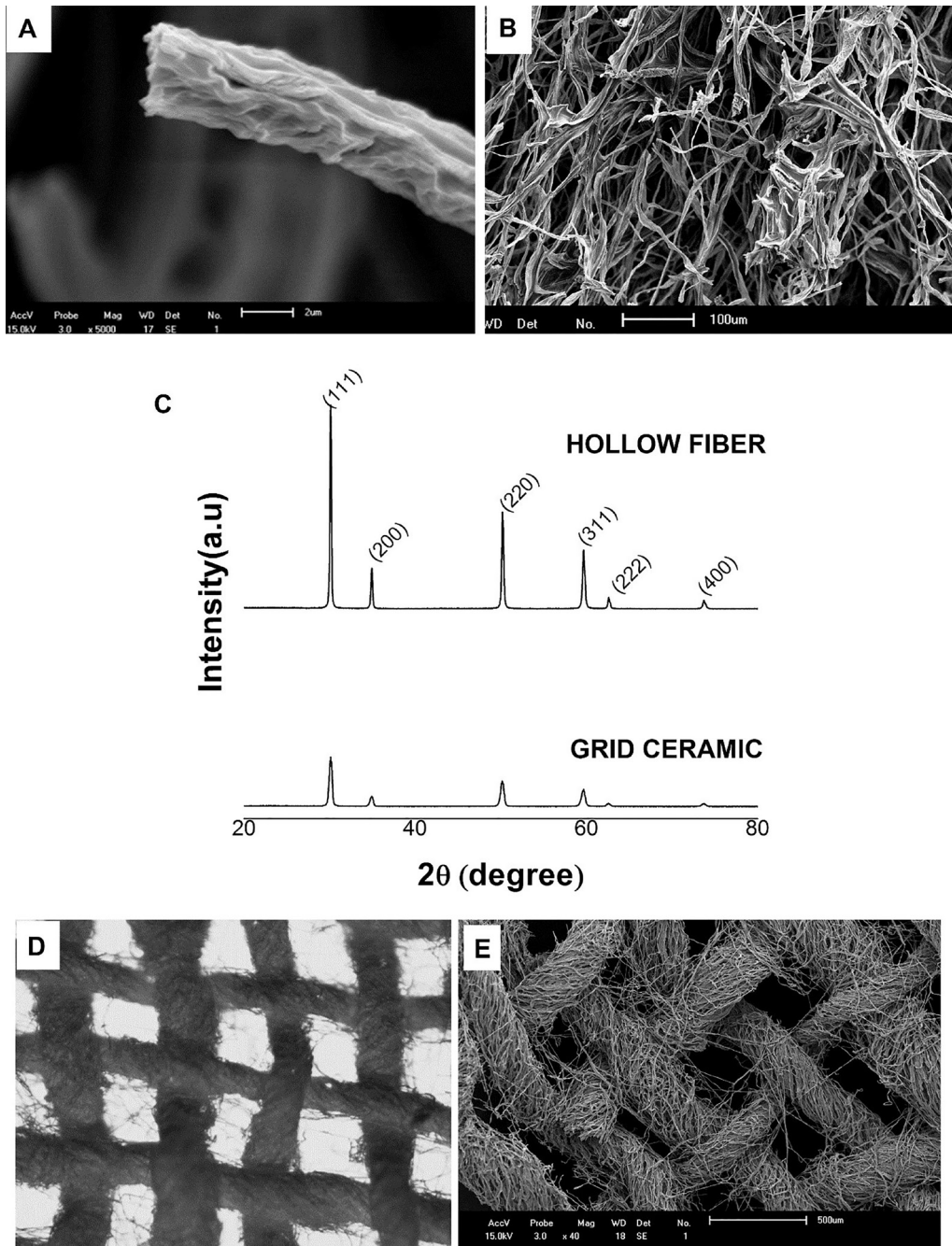


Figure 3. (A)(B)(C)(D) SEM micrograph images of ZrO₂-stabilised Yttrium oxide hollow fiber membranes at 800 °C for 3 h and (C) XRD pattern of cotton of ZrO₂-stabilised Yttrium oxide hollow fiber membranes.

Table 1: Sample characterization by N₂ adsorption annealing at 1000°C for 3h.

| Template annealing at 1000°C | SBET (m ² /g) | V _p (cm ³ /g ⁻¹) | d _{pore BJH} (Å) | d Average pore (Å) | Characterization of porous |
|------------------------------|--------------------------|--|---------------------------|--------------------|----------------------------|
| Cotton fiber YSZ | 9.94 | 0.008 | 31.55 | 79.73 | Behavior of Mesoporous |
| Cotton grid YSZ | 120.40 | 0.097 | 22.66 | 51.02 | Microporous |

V_p = pore volume at P/P₀ 0.994; d_{pore BJH} = BJH Method Desorption Pore Diameter; d_{pore} = Average Pore Diameter; S_{BET} = Specific Surface area determined by N₂ adsorption.

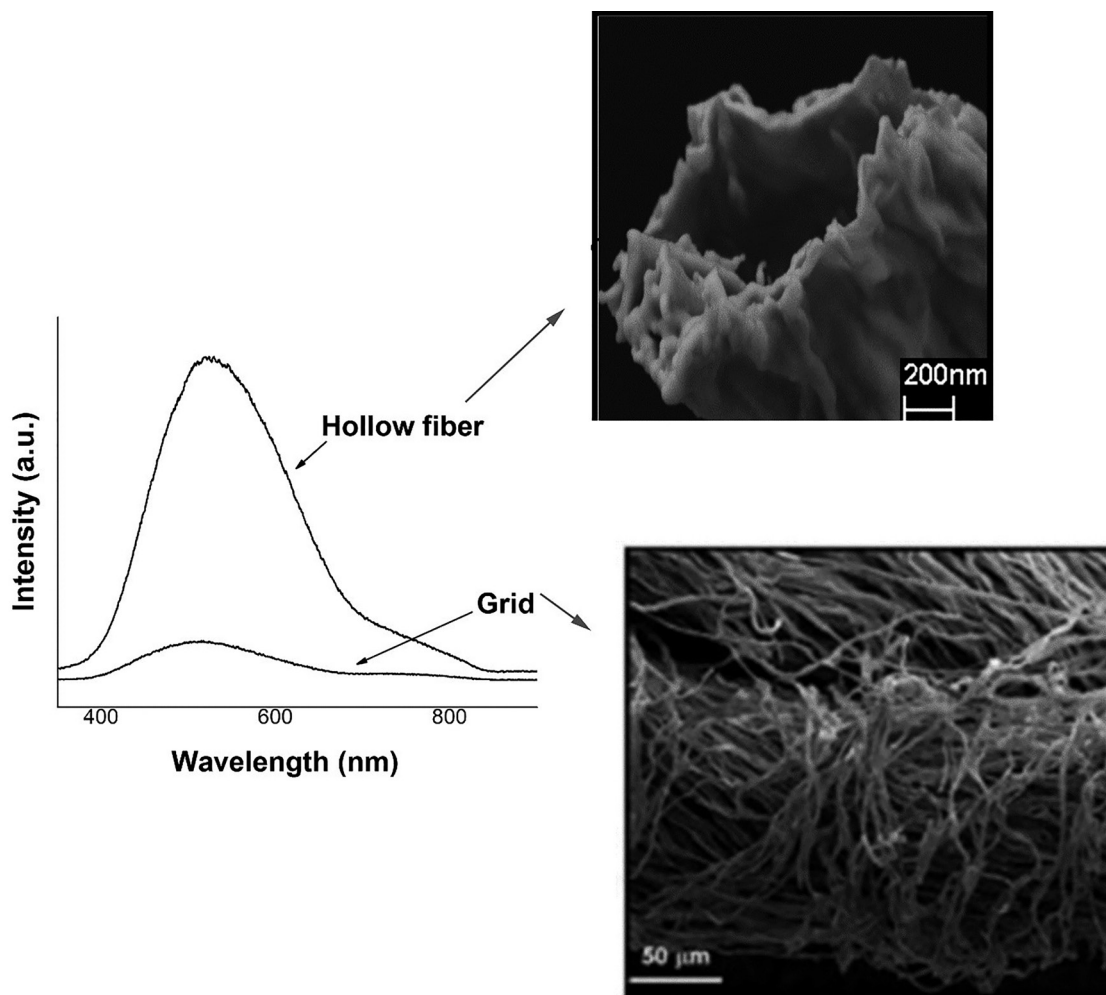


Figure 4. Photoluminescence at room temperature ($\lambda_{exc} = 350.7$ nm) of samples of fiber and grid ceramic at heat-treatment at 1000 °C for 3 h.

hydroxyapatite obtained from the organic template card when compared with the other shapes (hollow fibers and grid), fact related to the infiltration process (resin precursor) and subsequent burning organic template. The same material can be processed at the lowest scale through the appropriate organic templates (see Figure 6a). Hydroxyapatite fillers have known their applications illustrated here by the functionalization with the Agar (a natural polymeric). A transparent polymeric composite is illustrated in Figures 6b-c, which responded as a potential reinforced material. The fiber incorporation (0.5-2.0% by weight) into Agar polymer matrix increased significantly more than 25% the tensile strain of the pure material. There are reports of a 35% increase in Young's modulus (elastic modulus) and 25% in tensile strength by the addition of HA nanoparticles in the polymeric matrix¹⁹.

Concerning the ZT-nws samples, after membrane deposition and thermal treatment steps, the silicon substrate maintained the characteristic shiny finish of the polished surface with minimal tone variation, indicating

a good adhesion of the oxide to the substrate. The XRD analysis reveals the manifestation of weak peaks that can be associated with a $ZrTiO_4$ orthorhombic crystal system (JCPDS N_0 : 00-034-0415). Table 2 shows the (hkl) diffraction planes and the respective estimated 2θ Bragg positions for the ZT-nw diffraction planes. The medium intensity diffraction peak centered at 30.4° is assigned to the 100% peak of the orthorhombic $ZrTiO_4$ polycrystalline oxide. Despite the low intensity and presence of noise in the x-ray diffraction profile, some peaks could be assigned to the ZT-nw planes on the silicon wafer. XRD of the $ZrTiO_4$ powder obtained from thermal treatment at 700 °C of the same precursor polymer deposited on the membranes was performed to confirm the crystalline phase of the final material (Figure 7b). The presence of three sharp peaks at 38.11° , 44.32° and 64.45° are associated with the silver electrical contact applied to the sample in the FESEM experiments. The broad and intense peak in the $65-72^\circ$ 2θ range centered at 69° is related to the silicon wafer.

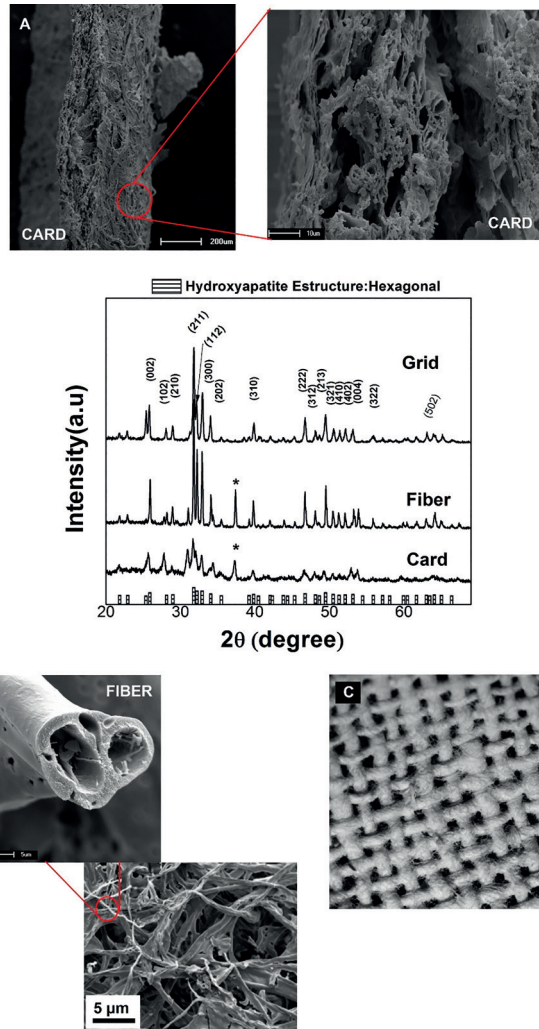


Figure 5. XRD and SEM images of (A) Card, (B) Fiber cotton, (C) Grid shape template of hydroxyapatite at 600 °C for 3 h.

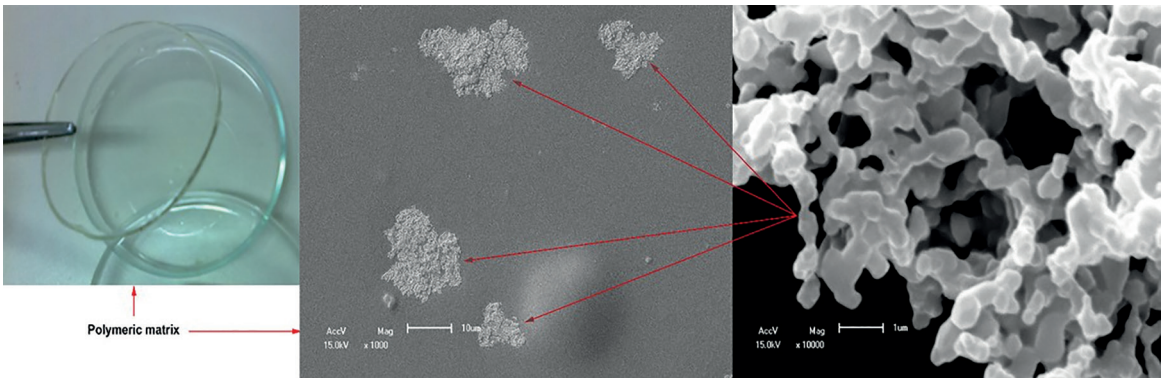


Figure 6. SEM images of hydroxyapatite fiber embedded in polymeric matrix.

Figure 7c and 7d shows the FESEM images of the ZT-nws, where one can observed that $ZrTiO_4$ nanowires were formed with a reasonable level of organization, producing high density regions of ZT-nws. Nanowires diameter (d) and length (l) were measured in electron microscopy images by

comparative analysis with the standard ruler. Nanowires are distributed in the substrate and show a mean aspect ratio (l/d) of approximately 30, the visual example show the diameter in nanometer scale.

Table 2: Estimated peak 2θ Bragg positions of diffraction planes (hkl) of the ZT-nws.

| (hkl) | 2θ Bragg from experimental observation | 2θ Bragg from JCPDS Card |
|---------|---|---------------------------------|
| (011) | 23.4 | 24.61 |
| (111) | 30.4 | 30.44 |
| (200) | 35.8 | 35.64 |
| (201) | 40.3 | 40.43 |
| (121) | 42.3 | 41.91 |
| (202) | 52.6 | 52.63 |
| (013) | 60.4 | 60.17 |
| (311) | 61.0 | 61.79 |

The membrane template-assisted methods require good wettability between the precursor solution and the templates to ensure complete filling of the membrane pores. If the precursor solution has good wettability with the template membrane, the capillary forces drive the solution into the pores²⁰. Polycarbonate membranes start to soften at approximately 150 °C and melt at around 240 °C. The low thermal template stability could restrain the oxide nanostructure growth during annealing of the precursor solution due to the destruction of the porous structure of the template. By using the membrane-assisted polymeric precursor route this event was avoided due to the formation of a characteristic glassy organic precursor at temperatures below 200 °C, which anchors the oxide structure inside the pores before the collapse of the porous membrane. In addition, the smooth surface of the silicon substrate contributed significantly to maintaining the pore structure during the thermal treatment and to

the formation of the ZT-nws. On the other hand, the use of polymeric precursor allow obtain a simples route to replicate templates, therefore desirables ceramic material could be process to improve specific applications described in the literature²¹.

4. Conclusion

In summary, several shape and porosity of ceramic structures were prepared using the polymeric precursor methods, and their crystalline and optical properties were investigated. The XRD results of the synthesized materials confirm that stable phase of $t\text{-ZrO}_2$ is formed and role of template and annealing treatment. The possibility of better control of the PL emission in fiber system may be related here to template shape and its specific microstructure in ceramic membrane. The effective incorporation on Agar matrix polymer is a decisive factor to specific application and developing of a biofunctional material and other approaches. Membrane-assisted synthesis associated with the polymeric precursor method was used in synthesis of ZrTiO_4 nanowires with controlled chemical compositions and high aspect ratio on a silicon substrate. The wires exhibit pore formation as a result of the incomplete densification process. This approach could potentially be extended in the future to process many other functional multi-component oxides as polycrystalline 1D nanostructures. Additional hollow ceramic membranes synthesized here suggests an important material in technological applications such catalyst, sensor or semiconductor system.

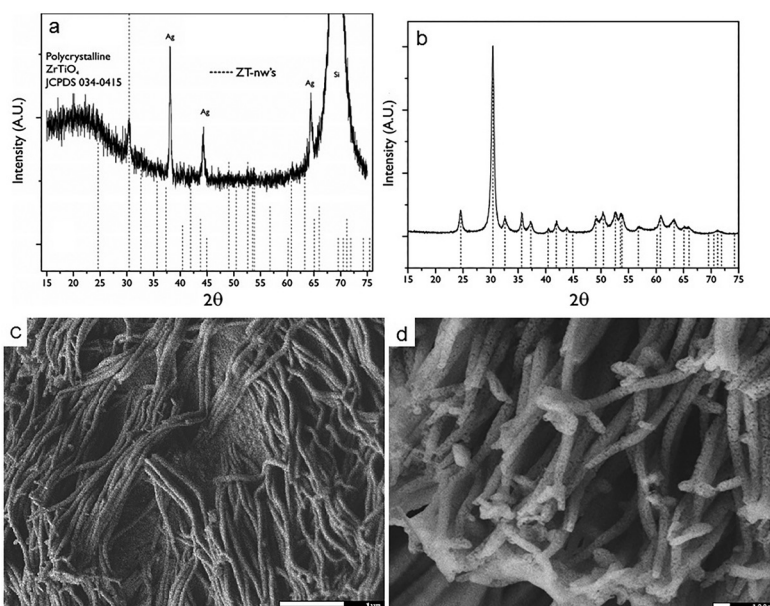


Figure 7. DRX patterns of (a) ZrTiO_4 nanowires on substrate; (b) ZrTiO_4 powder obtained from thermal treatment at 700 °C; (c) and (d) shows the FESEM images of the ZrTiO_4 nanowires.

5. Acknowledgment

The authors gratefully acknowledge the financial support of CNPq, process 482251/2013-1, CAPES and FAPERGS, process PQG 2013 002049-2551/13-2-1.

6. References

1. Azad AM. Fabrication of yttria-stabilized zirconia nanofibers by electrospinning. *Materials Letters*. 2006;60(1):67-72. DOI: 10.1016/j.matlet.2005.07.085.
2. Greil P. Advanced Engineering Ceramics. *Advanced Materials*. 2002;14(10):709-716. DOI: 10.1002/1521-4095(20020517).
3. Studart AR, Gonzenbach UT, Tervoort E, Gauckler LJ. Processing routes to macroporous ceramics: A review. *Journal of the American Ceramic Society*. 2006;89(6):1771-1789. DOI: 10.1111/j.1551-2916.2006.01044.x.
4. Tabata Y. Biomaterial technology for tissue engineering applications. *Journal of the Royal Society Interface*. 2009;6(Suppl 3):S311-S324. DOI: 10.1098/rsif.2008.0448.
5. Choi YC, Kim J, Bu SD. Template-directed formation of functional complex metal-oxide nanostructures by combination of sol-gel processing and spin coating. *Materials Science and Engineering: B*. 2006;133(1-3):245-249. DOI: 10.1016/j.mseb.2006.06.034.
6. Hulteen JC, Martin CR. A general template-based method for the preparation of nanomaterials. *Journal of Materials Chemistry*. 1997;7:1075-1087. DOI: 10.1039/A700027H.
7. Martin CR. Nanomaterials: A Membrane-Based Synthetic Approach. *Science*. 1994;266(5193):1961-1966. DOI: 10.1126/science.266.5193.1961.
8. Watanabe H, Kunitake T. Spatial Disposition of Dye Molecules within Metal Oxide Nanotubes. *Chemistry of Materials*. 2008;20(15):4998-5004. DOI: 10.1021/cm800549n.
9. Chung YA, Lee CY, Peng CW, Chiu HT. Reactive template assisted growth of one-dimensional nanostructures of titanium dioxide. *Materials Chemistry and Physics*. 2006;100(2-3):380-384. DOI:10.1016/j.matchemphys.2006.01.018.
10. Hua Z, Yang P, Huang H, Wan J, Yu ZZ, Yang S, et al. Sol-gel template synthesis and characterization of magnetoelectric $\text{CoFe}_2\text{O}_4/\text{Pb}(\text{Zr}_{0.52}\text{Ti}_{0.48})\text{O}_3$ nanotubes. *Materials Chemistry and Physics*. 2008;107(2):541-546. DOI: 10.1016/j.matchemphys.2007.08.023.
11. Kim J, Yang SA, Choi YC, Han JK, Jeong KO, Yun YJ, et al. Ferroelectricity in Highly Ordered Arrays of Ultra-Thin-Walled $\text{Pb}(\text{Zr,Ti})\text{O}_3$ Nanotubes Composed of Nanometer-Sized Perovskite Crystallites. *Nano Letters*. 2008;8(7):1813-1818. DOI: 10.1021/nl080240t.
12. Vakifahmetoglu C. Fabrication and properties of ceramic 1D nanostructures from preceramic polymers: a review. *Advances in Applied Ceramics: Structural, Functional and Bioceramics*. 2011;110(4):188-204. DOI: 10.1179/1743676111Y.0000000007.
13. Lucena PR, Pessoa-Neto OD, Santos IMG, Souza AG, Longo E, Varela JA. Synthesis by the polymeric precursor method and characterization of undoped and Sn, Cr and V-doped ZrTiO_4 . *Journal of Alloys and Compounds*. 2005;397(1-2):255-259. doi:10.1016/j.jallcom.2004.11.070.
14. Raubach CW, Krolow MZ, Mesko MF, Cava S, Moreira ML, Longo E, et al. Interfacial photoluminescence emission properties of core/shell $\text{Al}_2\text{O}_3/\text{ZrO}_2$. *CrystEngComm*. 2012;14(2):393-396. DOI: 10.1039/C1CE06099F.
15. Smith RM, Zhou XD, Huebner W, Anderson HU. Novel yttrium-stabilized zirconia polymeric precursor for the fabrication of thin films. *Journal of Materials Research*. 2004;19(9):2708-2713. DOI: http://dx.doi.org/10.1557/JMR.2004.0352.
16. Lucena PR, Prado WA, Braga VS, Carreño NLV. ZrTiO_4 nanowire growth using membrane-assisted Pechini route. *The Electronic Journal of Chemistry*. 2014;6(Suppl.1):QI-03. DOI: 10.17807/orbital.v6iS.1.655.
17. Hanaor DAH, Sorrell CC. Review of the anatase to rutile phase transformation. *Journal of Materials Science*. 2011;46(4):855-874. http://dx.doi.org/10.1007/s10853-010-5113-0.
18. Yang D, Qi L, Ma J. Hierarchically ordered networks comprising crystalline ZrO_2 tubes through sol-gel mineralization of eggshell membranes. *Journal of Materials Chemistry*. 2003; 13(1):1119-1123. DOI: 10.1039/b301077e.
19. Buczynska J, Pamula E, Blazewicz S. Mechanical properties of (poly (L-lactide-co-glycolide))-based fibers coated with hydroxyapatite layer. *Journal of Applied Polymer Science*. 2011;121(6):3702-3709. DOI: 10.1002/app.34189.
20. Cao G, Liu D. Template-based synthesis of nanorod, nanowire, and nanotube arrays. *Advances in Colloid and Interface Science*. 2008;136(1-2):45-64. DOI: 10.1016/j.cis.2007.07.003.
21. Santana BP, Paganotto GFR, Nedel F, Piva E, Carvalho RV, Nör JE, et al. Nano-/microfiber scaffold for tissue engineering: Physical and biological properties. *Journal of Biomedical Research. Part A*. 2012;100A(11):3051-3058. DOI: 10.1002/jbm.a.34242.